Computer simulation of the aggregation process in self-associating polymer and surfactant systems

Amitabha Chakrabarti and Raul Toral[a)]
Department of Physics and Center for Polymer Science and Engineering, Lehigh University, Bethlehem, Pennsylvania 18015

(Received 15 May 1989; accepted 18 July 1989)

We present results of numerical simulations of a new model for the clustering process in self-associating polymer systems. We focus on two experimentally interesting systems; telechelic ionomers and reverse micelles. The clustering dynamics introduced by us is an extension of the Eden method, previously used in the context of single particle aggregation. The structure of the aggregates seen in the simulations is qualitatively similar to that observed in experimental systems. The quantitative predictions of the model are found to be similar to those found in simulations of a model based on a diffusion-limited-aggregation-type process.

I. INTRODUCTION

Aggregation of self-associating polymer systems is of considerable current research interest,[1] mainly because of their unusual macroscopic material properties. In these systems, long flexible chain molecules, which have one or more associating sites, attract each other and in the process form clusters of characteristic geometry. One process of long standing interest is the aggregation of ionic polymers[2–6] or ionomers, in which clusters form via attraction between the ionic groups. Despite substantial experimental studies, neither the dynamics of self-association, nor the morphology of the corresponding aggregates is well known. The self-assembling process in the formation of miscelles[7–9] and reverse micelles[8,10–11] is also of increasing research interest. Micellar clusters are formed from surfactant molecules which contain both hydrophilic and hydrophobic groups. In micellar aggregates in aqueous solutions, the hydrophobic ends of the long chains form the core of the structure whereas the hydrophilic ends circle the core. On the other hand, in nonpolar solutions the structure of the aggregates is the reverse of that seen in aqueous solutions and, hence, they are named "reverse" micelles. Again, the details of the formation of reverse micelles and the size, shape, and stability of the corresponding clusters are not well known. At this stage, it seems that computer simulations of simple model systems which contain the essentials of the clustering process can play a major role in the theoretical understanding of these problems. While complete reproduction of experimental results can not be achieved in a simple model, one should still be able to identify the important features that contribute to the aggregation process and to the macroscopic properties by comparing the results of these models to experimental systems.

Recently, in two related papers,[12,13] Balazs and coworkers have extended the well-known diffusion-limited-aggregation (DLA)[14] model, previously used to study single particle aggregation, to the clustering process of long-chain molecules with one or more associating sites (which are loosely called "sticker sites" in the literature). In this model, one new chain at a time is released at a far distance from a seed chain. The new chain, then, executes a random walk on a lattice until, eventually, one of its stickers finds another sticker site already belonging to the aggregate. The new chain is then incorporated into the aggregate. In Ref. 12 the authors have carried out a computer simulation of the model in two dimensions and have studied the aggregation of long flexible chains with one associating site located at each of the two chain ends. This particular location of the stickers is relevant for telechelic ionomers[15] in which ionic groups occur only at the two ends of the chains, as well as in mesophase formation in liquid crystals with disk-like molecules.[16] Reference 13 reports on the aggregation process of chains with a single sticker at one end of each chain. For sufficiently long chains, the authors obtain structures similar to reverse micelles with very few chains belonging to the aggregate, which is a typical characteristic of reverse micelles as seen in experiments.[8,17]

In the DLA models, an important concept is that of an "active zone," consisting of all the sites which can mediate aggregation. In the single particle DLA there is a screening effect, such that the active zone is located on the surface of the cluster. For chains with a small number of sticker sites, we note that, as the chain length increases, the relative number of sticker sites decreases. Consequently, the active zone, although still located at the surface of the cluster, consists only of some few selected sites. Hence, when a new chain is released and reaches the surface of the cluster, it still spends considerable amount of time in locating the active sites. It seems possible to simplify the model is such a way that the search for the active sites is more efficient, while still keeping the essentials of the aggregation process intact. The method we propose in this paper is an extension of the Eden cluster formation dynamics[18] used in the case of single particle aggregation. Here, the addition of a new chain to the already formed aggregate is achieved by a self-avoiding random walk which starts ar a neighboring site of one of the existing sticker sites, chosen at random. Although, it might seem that this process will generate clusters quite different in morphology from that found in the DLA model, we argue that for sufficiently long-chain molecules, steric hinderance will not allow the active zone to spread from the surface of the clus-

[a)] Permanent address: Department de Fisica, Unversitat de les Illes Balears, 07071 Palma de Mallorca, Spain.

 0021-9606/89/215687-07$02.10

ters, since it is quite unlikely to find enough vacant sites to place a long chain in the core of the cluster. This will produce an effective screening which, as in the case of DLA, will control the morphology of the aggregates. Thus, we expect that our simplified model will be able to reproduce quantitatively most of the features seen in the DLA model and in experiments. The excluded volume effect generated by the long chains is *essential* to the equivalence of the two dynamical processes. For instance, we note that for single particle aggregation the Eden clusters are compact and the radius of gyration R_g for such a cluster in two dimensions scales as

$$R_g \propto N_e^{1/2}, \tag{1}$$

where n_e is the number of particles in the cluster. On the other hand, the single particle DLA clusters are ramified and the radius of gyration for such clusters scales as

$$R_g \propto n_d^{0.6}, \tag{2}$$

where n_d is the number of particles in a DLA cluster in two dimensions.

In order to check the abovementioned ideas of equivalence between DLA and Eden dynamics for long-chain molecules, we have carried out an extensive computer simulation in two dimensions. We found that, indeed, both models share universal features, such as that the exponents characterizing the radius of gyration of the aggregates are similar in both models. In addition, the simpler nature of the Eden-type dynamics makes the new model computationally more efficient and one can substantially reduce the statistical errors by simulating larger aggregates and by making averages over more "runs" in the same amount of available computer time as used in the DLA formulation.

The rest of the paper is organized as follows: in Sec. II we describe the model and the method of numerical calculations. In Sec. III we present the results for the aggregation of telechelic ionomers, and in Sec. IV we present the correspondig results for the reverse micelles. In Sec. V we conclude with a brief summary and related discussion of the results and possible extensions of our work.

II. THE MODEL AND NUMERICAL PROCEDURE

A telechelic ionomer chain is modeled by a self-avoiding random walk of $n-1$ bonds (correspondingly, n beads) in a square lattice, the two stickers being located at the two ends of the chain. We simulate the aggregation of telechelic ionomers by first placing a seed chain with one of its stickers located at coordinates $(L/2, L/2)$ of an $L \times L$ square lattice. The length of the lattice L is chosen with care such that the formed aggregate is always confined within the $L \times L$ geometry. All the chains in the simulation are constructed to obey the excluded volume criterion, so that a lattice site can not be occupied by more than one chain at any given instant of time. After placing the first chain in the matrix, we pick a bead randomly from that chain. If the chosen bead corres ponds to one of the stickers, we try to put a new chain (given again by a self-avoiding random walk) starting at a randomly chosen empty nearest-neighbor site of the sticker site. If, on the other hand, a nonsticking bead located at $\mathbf{r}_i$ is chosen, the chain dynamics is simulated by using the Verdier–Stockmeyer algorithm,[19] i.e., the new trail position of $\mathbf{r}_i$ is given by

$$\mathbf{r}_i' = \mathbf{r}_{i+1} - \mathbf{r}_i + \mathbf{r}_{i-1}, \tag{3}$$

where $\mathbf{r}_{i+1}$ and $\mathbf{r}_{i-1}$ are the locations of the $i+1$th and $i-1$th beads, respectively. The trial position $\mathbf{r}_i'$ is accepted only if it is not already occupied by any other chain molecule. One should also note that the chain motion depends on the local conformation of the chosen bead as well. When there is more than one chain present in the cluster, we first randomly choose a chain and then choose a random bead from this already selected chain. The aggregation process continues until there are a prescribed number of chains present in the cluster.

The model and the numerical procedure for the aggregation process of reverse micelles are similar to the above case, except for the fact that, in this case, the aggregating polymer chains contain only one sticker site at one of the ends. The presence of only one sticker per chain, however, radically alters the structure of the aggregates. In this particular growth process the excluded volume effect between the long tails limits the size of the aggregates. As the cluster grows, further addition of chains becomes more and more difficult and eventually the growth process stops and the cluster *freezes* with only a small number of chains belonging to it.

III. AGGREGATION OF TELECHELIC IONOMERS

Figures 1(a), 1(b), and 1(c) show the morphology of the aggregates with $n = 5$, $n = 25$, and $n = 50$, respectively. We note the presence of a gel-type spatially extended network even for very long chains. Actually, one can put as many chains in the cluster as one wants to, if the simulation continues for a long enough time. The global nature of these structures is similar to those observed in Ref. 12, although we note that in the latter case the aligning "tails" are designed to be adjacent and parallel to the tail of the nearest chain.

In analogy with single particle aggregation clusters, one would like to study the scaling law connecting the radius gyration R_g and the mass of the cluster nN, where N is the number of chains with n beads in the cluster. However, as discussed in Ref. 12, mass alone is inappropriate to be used as a single variable, since the entropy of the aggregating chains plays an important role in deciding the size and shape of the growing cluster. One thus expects that R_g depends on n and N separately, i.e.,

$$R_g \propto n^{\alpha} N^{\beta}. \tag{4}$$

A classical Flory-type theory[20] would predict[12] $\alpha = 3/4$ and $\beta = 1/2$ in two dimensions.

In order to calculate the exponent α we calculate the radius of gyration of a 100 and a 200 chain cluster for various values of the chain length between $n = 5$ and $n = 50$. The corresponding $\log R_g$–$\log n$ plots are shown in Fig. 2. The straight lines are the best fit to the data yielding $\alpha = 0.65 \pm 0.01$ in each case. interestingly enough, we note that this value of α is close to the value found in Ref. 12 in the "concentrated limit" (0.699 ± 0.008).

The exponent β is calculated in the following way: We fix the value of n and find the radius of gyration when the

FIG. 1. (a) A typical morphology for the aggregates for telechelic ionomers for $n = 5$. There are 200 chains in the cluster. A polymer chain is represented here as a series of connected sites on a square lattice. The two sticker sites at the ends of the chains are represented by bold dots. (b) Same as (a) for $n = 25$. There are 100 chains in the cluster. (c) Same as (a) for $n = 50$. There are 100 chains in the cluster.

number of chains belonging to the cluster is varied from 10 to 4000 (the maximum number of chains put in the clusters is 1000 for $n = 5$ and $n = 10$, and 4000 for $n = 20$). Our results for $n = 5$, 10, and 20 yield $\beta = 0.44 \pm 0.01$, $\beta = 0.45 \pm 0.01$, and $\beta = 0.46 \pm 0.01$, respectively. In Fig. 3 we plot $\log (\mathbf{R}_g/n^{\alpha})$ vs $\log N$ (with $\alpha = 0.65$) for $n = 5$, 10, and 20. The collapse of all the data on a single master curve emphasizes that Eq. (4) describes the correct scaling behavior of the growth process. A straight line with a slope 0.45 is also included in Fig. 3 as a guide to the eye. We note that a similar value of the exponent β (0.450 ± 0.009 in the concentrated regime) was found in Ref. 12. For compact clusters in two dimensions one expects $\beta = 0.5$. The authors of Ref. 12 argued that the lower value of the exponent β found in their simulations can be explained by the presence of self-loops which cause the cluster to contract. We believe, though, that the reason for β being less than 0.5 is simply due to the fact that the size of the clusters studied in the simulations are not large enough to enter the asymptotic scaling regime and $\beta = 0.5$ will be recovered for sufficiently large N which, however, is more demanding on the computer resources.

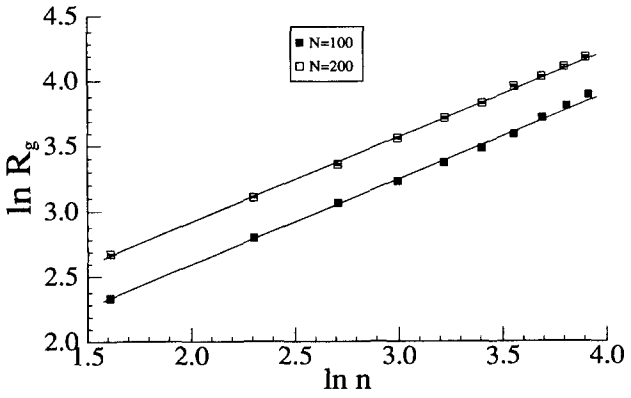

FIG. 2. Logarithmic plot of radius of gyration (R_g) vs number of beads (n) for 100 and 200 chain telechelic ionomer clusters. The straight lines are the best fit to the data yielding the slope as 0.65 ± 0.01.

IV. FORMATION OF REVERSE MICELLES

In this study we investigate two limits; short chains ($\leqslant 5$ beads) and long chains ($\geqslant 15$ beads). For short chains we show the morphology of the clusters in Figs. 4(a), 4(b), and 4(c). The spatially extended structures for small chain lengths are clear from these figures. The radius of gyration of these clusters for fixed value of n ($= 2,3,5$) and different values of N are presented in Figs. 5(a), 5(b), and 5(c), respectively. We note that although the morphology of the clusters seems ramified as seen in the Figs. 4 one finds that the exponent β, defined by

$$R_g \propto N^{\beta} \tag{5}$$

is very close to 0.5 as expected for ordinary Eden clusters.

The dramatic influence of increased chain length is demonstrated in Figs. 6(a), 6(b), and 6(c), where chain lengths of $n = 15$, $n = 25$, and $n = 50$ are shown. Similar to the conclusions of Ref. 13 we find that there is a critical chain length n_c (somewhere between $n = 5$ and $n = 15$), such that for $n < n_c$ the chains form spatially extended network resembling a lamellar phase and for $n > n_c$ the excluded volume effect sterically hinders more chains to be attached to the

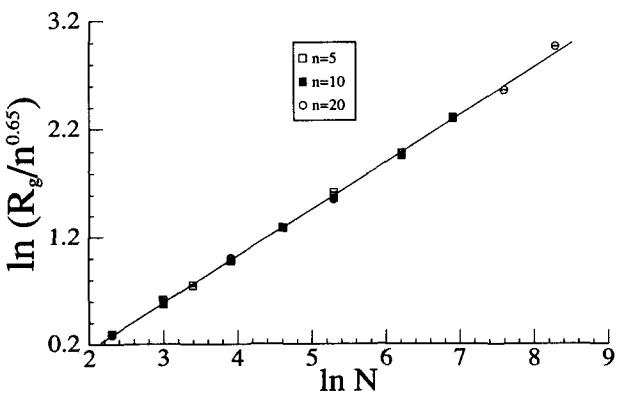

FIG. 3. Logarithmic plot of radius of gyration (R_g) scaled by n^{α} ($\alpha = 0.65$) vs number of chains (N) for chain length $n = 5$, $n = 10$, and $n = 20$ in the case of telechelic ionomer clusters. The maximum number of chains put in the clusters is 1000 for $n = 5$ and $n = 10$, and 4000 for $n = 20$. The straight line with a slope of 0.45 is a guide to the eye.

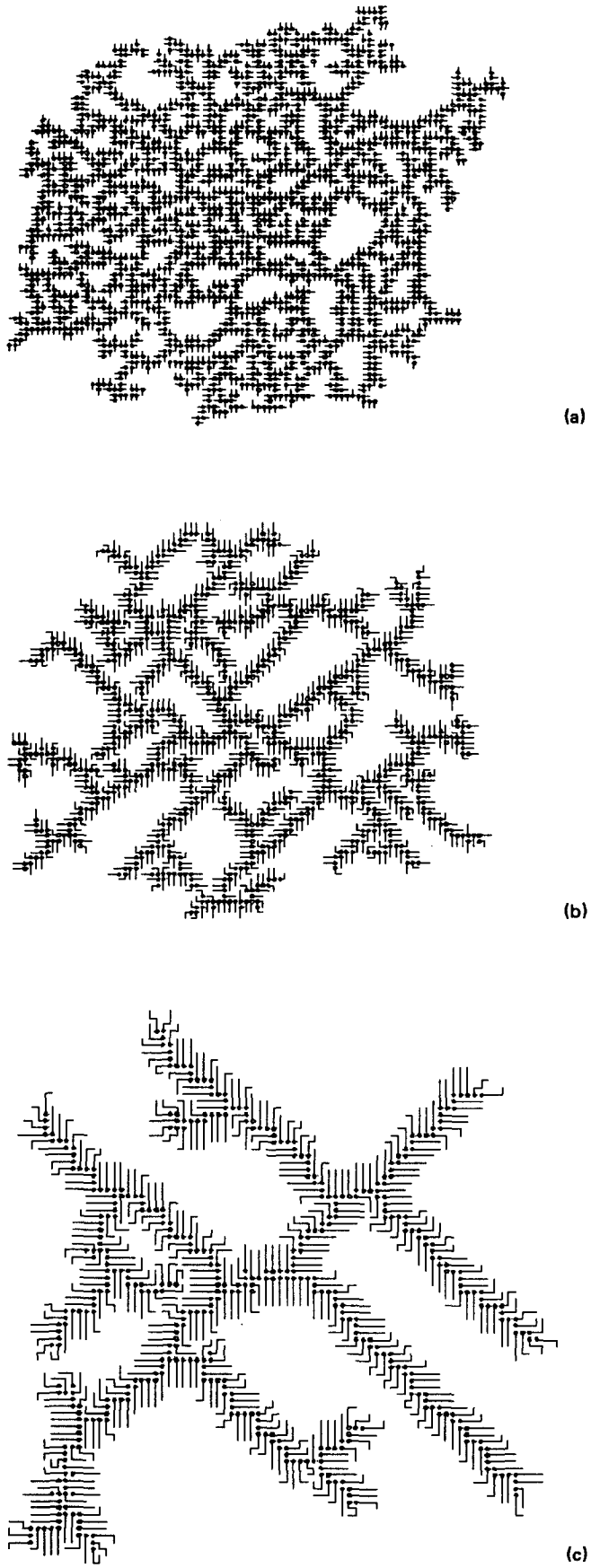

FIG. 4.(a) A typical morphology for the aggregates for short chains ($n = 2$) with one sticker site. There are 2000 chains in the cluster. (b) Same as (a) with $n = 3$. There are 1000 chains in the cluster. (c) Same as (a) with $n = 5$. There are 500 chains in the cluster.

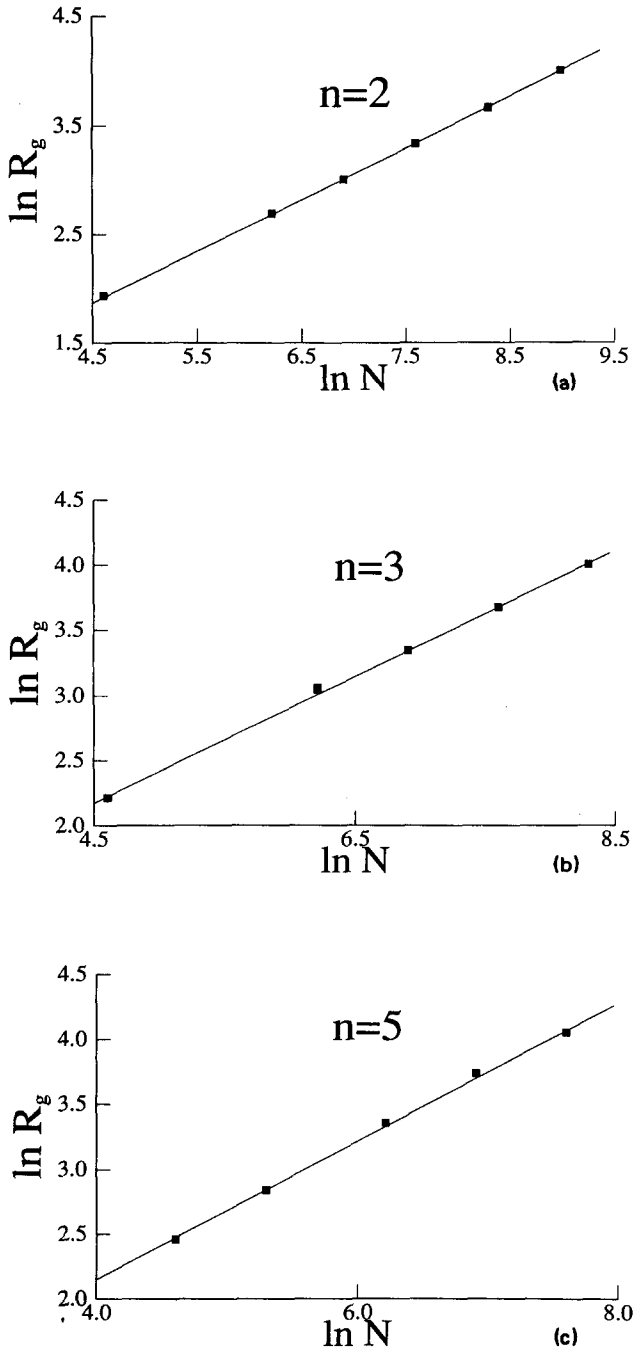

FIG. 5. (a) Logarithmic plot of radius gyration (R_g) vs number of chains (N) for chain length $n = 2$ in the case of aggregates for short chains with one sticker site. The straight line is the best fit to the data yielding the slope as 0.48 ± 0.02. (b) Same as (a) for chain length $n = 3$. The straight line is the best fit to the data yielding the slope as 0.49 ± 0.02. (c) Same as (a) for chain length $n = 5$. The straight line is the best fit to the data yielding the slope as 0.52 ± 0.02.

cluster and the clusters freeze eventually. For large n, the clusters contain only a few chains and are circular in shape. We note that when tail groups are significantly larger than the head groups, micelles appearing circular in cross section are seen in experimental studies.[8] Also, it is a remarkable feature that the relatively small size of the aggregates seen in experiments is reproduced in our simulations for long chains. It is interesting to find a scaling relation between the number of chains N_f in a frozen cluster and the length of the chains n in the cluster. Figure 7 shows a log–log plot of N_f vs n. From this figure it seems that

$$N_f \propto n^{-\gamma}, \tag{6}$$

where our estimate for γ is $\gamma = 1.7 \pm 0.1$. This value of γ is somewhat different from that found in Ref. 13 ($\gamma = 1.14$). However, we note that in Ref. 13 attracting sites can occupy the first and second nearest-neighbor sites, whereas in our case the connectivity is restricted to only nearest-neighbor sites. This could be a possible reason that the value of γ found here is larger than in Ref. 13. We also point out that an accurate determination of the average number of chains in a frozen cluster is a computationally difficult task, because of the large fluctuations associated with this quantity. This fact shows up as large error bars in the data shown in Fig. 7 even after averaging over 50 runs (in Ref. 13 averages were made only over 5 runs). Also, the length of chains varies only from 15 to 25 in this study and it may not be enough to extract a meaningful exponent from data of this limited nature. However, working with samples containing larger chain lengths would take substantial amount of more computer time and even then, one would not totally solve the problem since the number of chains in a frozen cluster of larger chains is small and an accurate calculation is very difficult. Thus it is not totally clear at this point whether the difference in the γ values between the Eden-type and DLA-type models is physically significant or is entirely due to the difference in the local details of the two simulations. An analytical calculation of the size of the frozen clusters, however approximate, would be very useful to clarify this issue.

V. CONCLUSIONS

In this paper we have introduced a new model for the formation of self-associative polymer aggregates, focusing on aggregation of telechelic ionomers and formation of reverse micelles. The dynamics introduced by us is based on the one used previously in the context of the formation of Eden clusters. This method, although relatively simple, qualitatively reproduces structures observed in experimental systems. The quantitative predictions of the model, as determined by different exponents characterizing morphology and compactness of the structures, are also found to be similar to those obtained in simulations of a model based on a DLA-type dynamics.

One can possibly argue, though, that the use of the Eden model in the present context is based on the assumption that the rate limiting process is the reaction between the sticker sites, whereas in DLA-type dynamics the growth process is limited by the diffusion of the reactive chain to the surface of the growing cluster. However, we note that in DLA-type simulations, the chains are allowed to associate only through the sticker sites (i.e., the interactions between the chains are assumed to be mediated *only* by the sticker sites) and as a consequence the rate limiting process also depends on the reaction of the sticker sites. Thus, for aggregation of long chain molecules with a few sticker sites these two dynamics are closer to each other than in the case of single particle

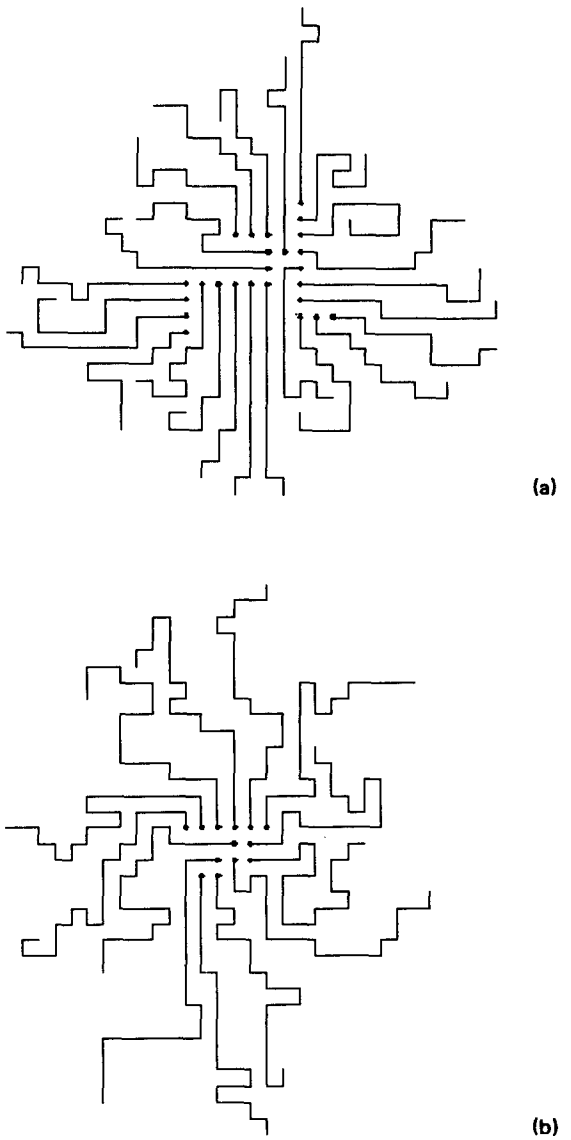

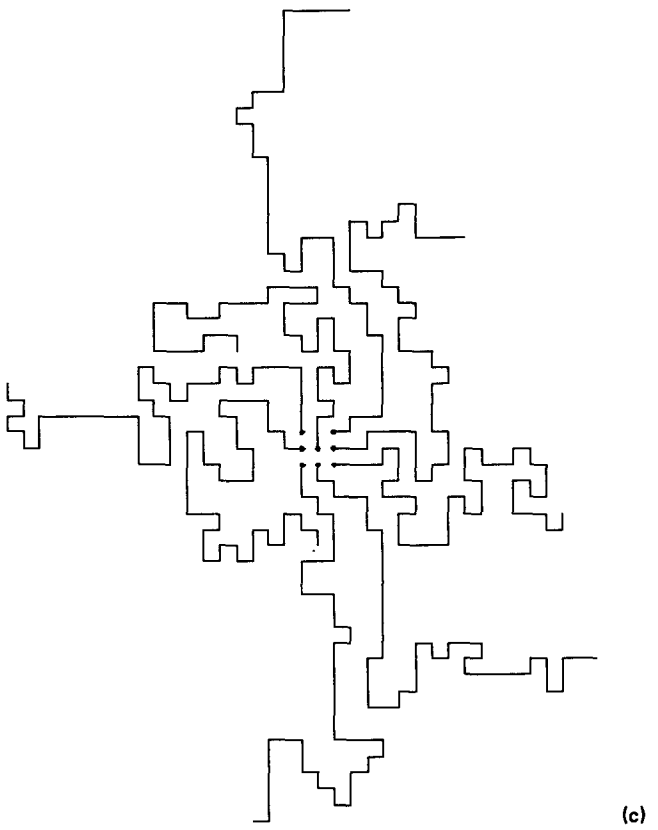

FIG. 6. (a) A typical morphology for the aggregates for reverse micelles with chain size $n = 15$. There are 24 chains in the cluster. (b) Same as (a) with $n = 25$. There are 13 chains in the cluster. (c) Same as (a) with $n = 50$. There are 8 chains in the cluster.

aggregation. It turns out that the excluded volume effect is the most important constraint in designing the morphology, and thus the details of the particular dynamics used for the formation of the clusters become unimportant.

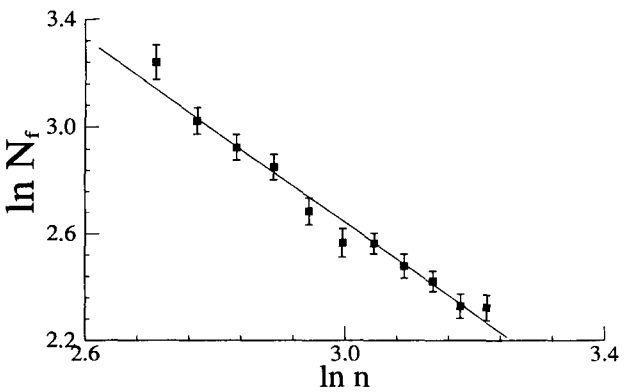

FIG. 7. Logarithmic plot of number of chains in a reversed micelle (N_f) vs the length of the chains (n). The straight line is the best fit to the data yielding the slope as -1.7 ± 0.1.

We are aware that the models presented in this paper, as well as the ones discussed in Refs. 12 and 13, are too simplistic in nature. In order to make these models more realistic we are currently extending the methods to study the more important case of aggregation in three dimensions where we assign probabilities to the sticking process which decrease with increasing separation between the sites and/or increasing the thermal fluctuations. The results will be reported elsewhere.[21]

ACKNOWLEDGMENTS

We thank Professor J. D. Gunton and Professor M. Muthukumar for many useful comments. This work was supported by NSF Grant No. DMR-8612609. R. T. also acknowledges financial support from DGICYT Project No. PB-86-0534 (Spain).

[1] J. N. Israelachvili, *Intermolecular and Surface Forces with Applications to Colloidal and Biological Systems* (Academic, New York, 1985).
[2] A. Eisenberg, Macromolecules **3**, 147 (1970).
[3] L. Holliday, *Ionic Polymer* (Halstead, New York, 1975).
[4] A. Eisenberg, and M. King, *Ion Containing Polymers* (Academic, New

York, 1977).
[5]I. Duvdevani, P. K. Agarwal, and R. D. Lundberg, Polym. Eng. Sci. **22**, 499 (1982).
[6]W. J. MacKnight and T. R. Earnest, Macromol. Rev. **16**, 41 (1981).
[7]J. H. Fendler and E. J. Fendler, *Catalysis in Micellar and Macromolecular Systems* (Academic, New York, 1975).
[8]H. F. Eicke, in *Micelles*, edited by M. J. S. Dewar (Springer, Berlin, 1980).
[9]F. Menger, Acc. Chem. Res. **12**, 111 (1979).
[10]Z. A. Schelly, in *Aggregation Process in Solution*, edited by E. Wyn-Jones, and J. R. Gormally, Elsevier, Amsterdam, 1983.
[11]*Reverse Micelles, Biological and Technological Relevance of Amphiphilic Structures in Apolar Media*, edited by P. L. Luisi and B. E. Straub (Plenum, New York, 1982).
[12]A. C. Balazs, C. Anderson, and M. Muthukumar, Macromolecules **20**, 1999 (1987).
[13]A. C. Balazs, F. E. Karasz, and W. J. MacKnight, Cell Biophys. **11**, 91 (1987).
[14]T. A. Witten and L. M. Sander, Phys. Rev. Lett. **47**, 1400 (1981); *Kinetics of Aggregations and Gelation*, edited by F. Family and D. P. Landau (North Holland, New York, 1984).
[15]E. J. Goethals, *Telechelic Polymers: Synthesis and Applications* (CRC, Boca Raton, 1989); R. D. Hegedus, Ph. D. thesis, University of Massachusetts, Cambridge, 1985 (unpublished).
[16]W. Kreuder, H. Ringsdorf, and P. Tschirner, Makromol. Chem., Rapid Commun. **6**, 367 (1985).
[17]J. H. Fendler, *Membrane Mimetric Chemistry* (Wiley, New York, 1982).
[18]M. Eden, in *Proceedings of the Fourth Berkeley Symposium on Mathematical Statistics and Probabilities*, edited by F. Neyman (University of California, Berkeley, 1961), Vol. IV. See also Ref. 14.
[19]P. H. Verdier and W. H. Stockmeyer, J. Chem. Phys. **36**, 227 (1962); C. Domb, Adv. Chem. Phys. **15**, 229 (1962); H. J. Hilhorst, and J. M. Deutch, J. Chem. Phys. **63**, 5153 (1975).
[20]P. J. Flory, *Principles of Polymer Chemistry* (Cornell University, Ithaca, New York, 1953); P. G. de Gennes, *Scaling Concepts in Polymer Physics* (Cornell University, Ithaca, New York, 1979).
[21]R. Toral and A. Chakrabarti (unpublished).